

Formation of Curved Seafloor Fabric by Changes in Rift Propagation Velocity and Spreading Rate: Application to the 95.5° W Galapagos Propagator

GARY ACTON AND SETH STEIN

Department of Geological Sciences, Northwestern University, Evanston, Illinois

JOSEPH F ENGELN

Department of Geology, University of Missouri, Columbia

The geometry of oceanic spreading centers can change by rift propagation, in which a new ridge segment propagates and preempts a preexisting one. As the locus of relative motion between the two plates shifts, the dying and growing ridge segments are joined by a boundary, usually a transform, which migrates with time, causing seafloor to be transferred from one plate to the other. As a result, originally ridge-parallel isochrons in a zone between the growing and failed rifts can be reoriented to trends oblique to both the ridge and spreading direction. An attractive feature of this model is that the reorientation occurs by strictly rigid plate tectonics, since relative motion occurs only between points on different plates. Recent surveys of the Galapagos propagating rift system at 95° W show seafloor fabric curving away from the growing rift and toward the failed rift. These observations have been interpreted as requiring a zone of distributed simple shear between the two rifts. Such behavior would represent a local deviation from rigid plate tectonics, since relative motion would be distributed over a finite region not part of either of the two plates. Here we explore possible rigid plate models for the formation of curved seafloor lineaments by rift propagation. We find that such fabric can be generated by changes either in the velocity (rate or direction) of rift propagation, or in the spreading rate during rift propagation. The curvature of various tectonic elements is diagnostic of the different possibilities. The geometry observed at the Galapagos can result from either rift propagation acceleration, or a spreading rate decrease, during the last few hundred thousand years. The reverse curvature could result from either deceleration of rift propagation or an increase in spreading rate. Propagator acceleration and spreading rate slowing, which produce similar structural trends, could in principle be distinguished using spreading rate data. At Galapagos, however, since either would have occurred within the present period of normal polarity, both are consistent with the magnetic anomaly data. We thus conclude that the data interpreted as requiring a shear zone are equally consistent with two distinct models based on rigid plate tectonics. It may, however, be possible to discriminate between rigid and shear models using fabric observations at other propagators. The shear model requires that the sense of curvature at Galapagos be a ubiquitous feature of active propagators. In contrast, the rigid plate tectonic model allows for fabric with a variety of orientations, including reverse curvature formed by either propagation deceleration or increasing spreading rate and linear fabric formed by constant propagation and spreading velocities.

It is hard to overstate the importance of the discovery that new seafloor forms in a zone only about 10 km wide. The narrowness of this zone plays an important role in the plate tectonic model for explaining the geology and geophysics of rises. It is the sharpness of this boundary that makes the paleomagnetic tape recorder possible and provides the basis of the simple geometrical relationships that make plate tectonics so useful.

Plate Tectonics: How It Works
Allan Cox and Robert B. Hart

INTRODUCTION

The basic premise of plate tectonics is that the relative motion of essentially rigid plates is concentrated in narrow zones along discrete boundaries [Morgan, 1968]. Active oceanic spreading centers, as summarized in the above quotation, are one of the most striking examples of such boundaries. Their geometry can change significantly with

time, as evidenced by the extinct spreading centers in the southeast Pacific shown by both residual topography and magnetic anomalies [Menard *et al.*, 1964; Herron, 1972a; Mammerrickx *et al.*, 1980]. The evolution of oceanic ridges has thus been a prime topic for investigation with plate tectonic models.

The propagating rift model for changes in spreading center geometry (Figure 1), developed to explain the origin of observed magnetic anomalies and structures oblique to both spreading center and transform fault trends [Hey, 1977; Hey *et al.*, 1980], has proved valuable. In this model a new ridge segment forms and propagates at the expense of an adjacent segment, which is preempted and ceases to spread. The locus of relative motion between the two plates shifts from the dying rift to the growing one, such that the rift tips are joined by a transform which migrates with time, transferring lithosphere from one plate to the other. The growth of the propagator thus results in characteristic seafloor structures. Distinct boundaries known as pseudofaults bound a wedge-shaped zone of seafloor formed at the propagating rift. Isochrons in the region of lithosphere transferred between plates, bounded by the failed rift trace and inner pseudofault, can be

Copyright 1988 by the American Geophysical Union

Paper number 7B3040
0148-0227/88/007B-3040\$05.00

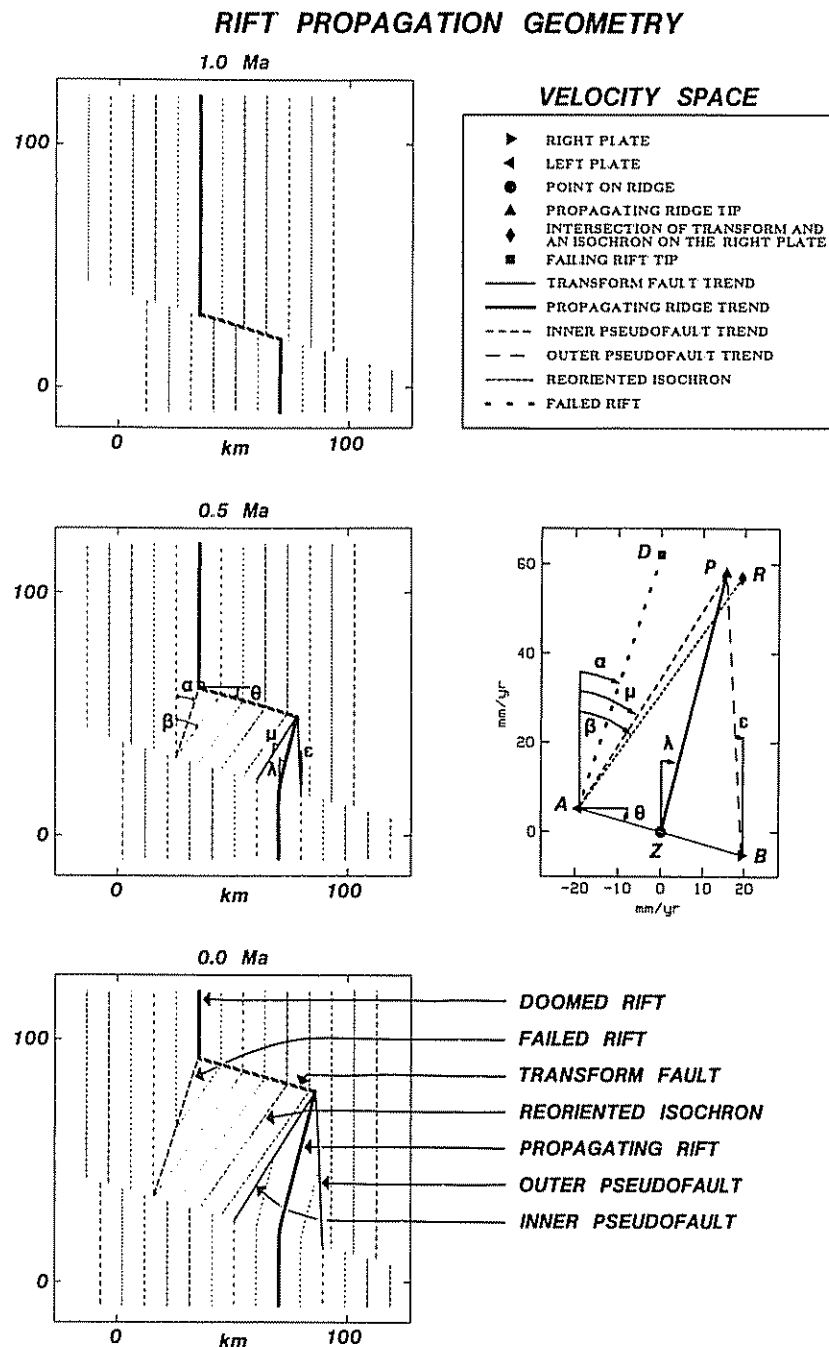


Fig 1 Geographic and velocity space representation for a simple steady state propagating rift. Rift propagation begins 1 Ma at the southern ridge-transform intersection and proceeds to the present (0 Ma) with constant propagation velocity (rate 60 mm/yr, direction N15° E) and spreading velocity (rate 20 mm/yr, direction N105° E). Isochrons are created every 0.5 m.y. During the evolution, relative motion shifts instantaneously from the dying to the growing rift. The instantaneous transform fault connecting the rift tips thus migrates to the northeast, transferring lithosphere from the right plate to the left. Labeled angles and points are listed in the notation list.

reoriented to trends differing from those of both the prepropagation seafloor fabric and the lithosphere formed during propagation. An attractive feature of the model is that the oblique structures resulting from the lineation reorientation form as a consequence of rigid plate tectonics because at any time, motion occurs only across discrete plate boundaries.

Rift propagation models have been used to describe the tectonic evolution of several areas, including the Gulf of Aden [Courtilot et al., 1980], the Juan de Fuca Ridge [Hey

and Wilson, 1982; Johnson et al., 1983; Wilson et al., 1984], and the Gorda Rise [Stoddard, 1987]. The best documented presently active example of this process is the Galapagos propagator at 95.5° W on the Cocos-Nazca spreading center (Figure 2). Bathymetric and magnetic data show a westward propagating rift preempting a failing rift to the south, and the associated structures predicted by the rift propagation model [Hey and Vogt, 1977; Searle and Hey, 1983; Hey et al., 1986; Miller and Hey, 1986].

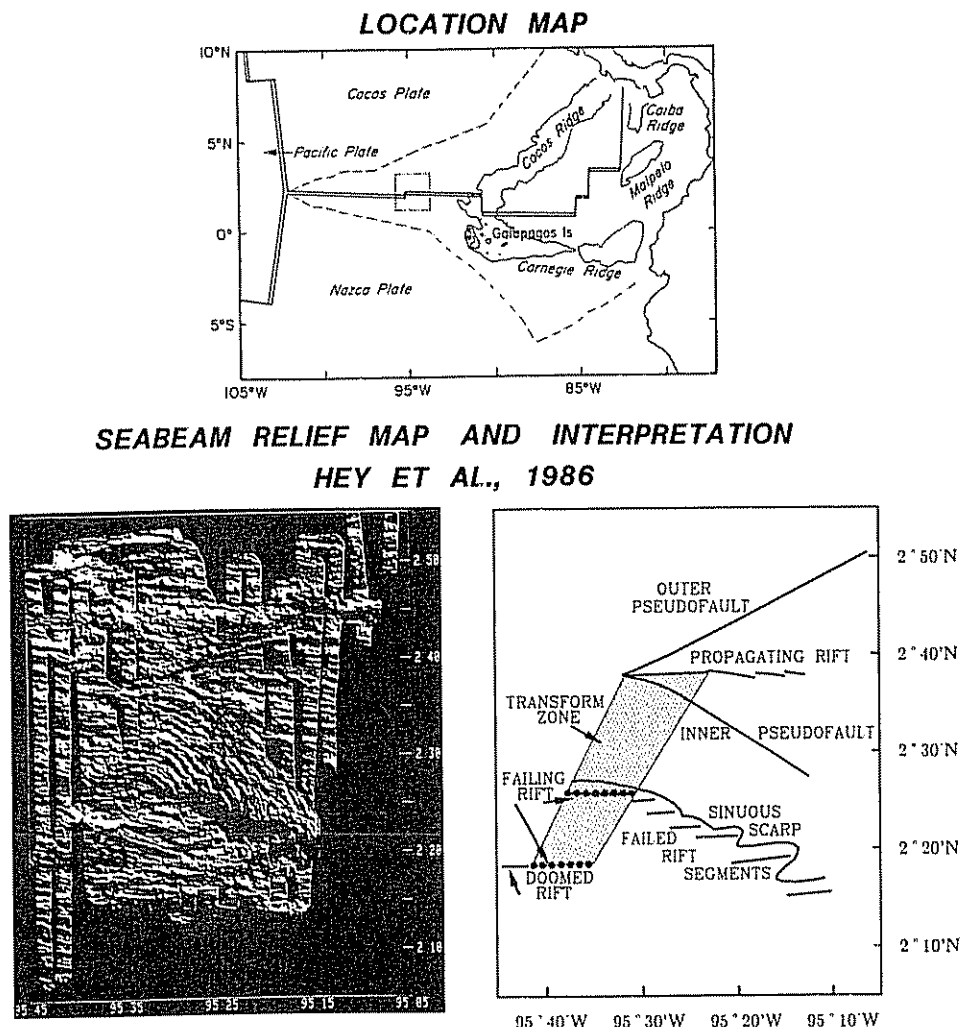


Fig. 2 Location and tectonics of the $95^{\circ} 5' W$ propagating rift (Top) Location map [Hey *et al.*, 1980]. (Bottom left) Sea Beam relief map of the region near the rift tip and (Bottom right) tectonic interpretation. Note the region of curved structures between the propagating and failed rifts

An interesting feature of the $95^{\circ} 5' W$ Galapagos propagator is the distinct curvature of the oblique fabric associated with the propagation, in contrast to the linear trends shown in Figure 1. Figure 2 shows an image of Sea Beam data over the rift tip area and its tectonic interpretation [Hey *et al.*, 1986]. Lineations in the zone between the scarp marking the failed rift trace and the inner pseudofault have curvature concave toward the failed rift. Hey *et al.* [1986] interpreted these data using a variation on the simple rift propagation model during which spreading is gradually rather than instantaneously transferred to the propagating rift, and shear occurs between the conjugate spreading centers during the finite length of time in which both are active [Hey *et al.*, 1980]. The curved lineations would mark a broad transform zone connecting the failing, but still active, rift to the propagating one. McKenzie [1986] has presented an analytic formulation for this process which reproduces the general features observed.

The shear zone model, which requires a deviation from rigid plate tectonics in an overlap region some tens of kilometers wide, has interesting implications for larger-scale spreading center reorientations. Two presently active examples occur along the East Pacific Rise where

the total Nazca-Pacific relative motion is divided between two active ridges separated by overlap regions hundreds of kilometers wide, known as the Easter and Juan Fernandez microplates [Forsyth, 1972; Herron, 1972b; Anderson *et al.*, 1974; Handschumacher *et al.*, 1981; Engeln and Stein, 1984; Naar and Hey, 1986; Schilling *et al.*, 1985; Hey *et al.*, 1985; Anderson-Fontana *et al.*, 1986; Engeln *et al.*, 1988; Francheteau *et al.*, 1987]. These presumably evolved by rift propagation, but interpretations differ as to whether the overlap regions between the growing and dying ridges behave as rigid microplates or shear zones. Rigid plate models are suggested by the concentration of seismicity along their boundaries [Forsyth, 1972] and the reasonable success of Euler vectors [Engeln and Stein, 1984; Anderson-Fontana *et al.*, 1986] derived from inversions of plate motion data (spreading rates, transform azimuths, and slip vectors) in both describing the available data and predicting those subsequently acquired. Observations of fabric within the Easter microplate oblique to the surrounding spreading centers are subject to differing interpretations. Hey *et al.* [1985] suggest that these data indicate that some shearing occurs; Engeln *et al.* [1988] find these data consistent with rigid plate tectonics.

The issue is thus on what length scale deviations from rigid plate tectonics need be invoked. It is therefore natural to ask whether the curved seafloor fabric at the Galapagos propagator requires the existence of a shear zone. In this paper, we discuss various rift propagation geometries that produce curved lineations due to the variation of propagation velocity (either rate or direction) and spreading rate over time. We then present two alternative models for the Galapagos propagator, one with accelerating propagation and one with decreasing spreading rates, which reproduce the observed structures. Both models require no shear zone and are consistent with rigid plate tectonics.

RIFT PROPAGATION GEOMETRY

We examine the conditions under which rift propagation can form curved structures, using a velocity space representation of a general propagation geometry (Figure 1 and notation list) [Engeln *et al.*, 1988], derived from one by Searle and Hey [1983]. This representation shows the orientation of the various structures produced by propagation, for given values of the spreading rate and azimuth, and the rate and direction of rift propagation. We predict the trends of both rifts, of isochrons formed on the growing rift, of the reoriented isochrons, of the inner and outer pseudofaults, and of the transform fault. It is thus possible to find spreading and propagation histories consistent with a given set of observed trends.

Propagation is assumed to begin at a ridge-transform intersection. We describe the geometry in a reference frame aligned with the doomed rift (or equivalently the original fabric) such that the x and y directions are normal and parallel to the doomed ridge trend, respectively. The relative plate motion is given by the half spreading rate u and obliquity θ (both measured with respect to the normal to the doomed rift), so the two plates are represented by points A and B with coordinates $(-u, u \tan \theta)$ and $(u, -u \tan \theta)$. The propagator moves at a velocity with components w normal to the doomed ridge and v parallel to it, so the propagator tip is at P (w, v) . The dead rift and reoriented isochrons are given by points D and R with coordinates $(0, v + w \tan \theta)$ and $(u, v + (w - u) \tan \theta)$. The resulting configuration can be described by several angles measured relative to the initial fabric. The propagator moves in the direction given by λ , the trends of the inner and outer pseudofaults, which enclose the seafloor formed on the propagating ridge, are μ and ϵ , and the failed rift trend is α . Due to seafloor transfer between the plates, originally ridge-parallel isochrons between the inner pseudofault and dead ridge are reoriented to trends β .

In Figure 1, for example, oblique spreading occurs on two N-S trending ridge segments. Propagation begins at the southern ridge-transform intersection and proceeds at a constant rate in a direction orthogonal to plate motion. Lithosphere is transferred from the right plate to the left as relative motion instantaneously shifts from the dying to the growing ridge. In this example, the ridge-normal component of propagation velocity is less than the half rate ($w < u$), so the rift tip propagates into successively younger seafloor. To see this, note that the lithosphere immediately outside the outer pseudofault gets younger toward the rift tip.

Consider the problem of reconstructing the past plate boundary configuration for this example, given the 0 Ma (present) "data." Since the propagation velocity and spreading rate and direction were assumed constant, the angular relations have not changed once propagation began. The spreading direction θ and ridge-normal half rate u are given by the transform and the isochrons formed during propagation. By combining these with the ratio of the propagation velocity components indicated by the new rift trend λ and one of the other angles, both components can be found. We will see, however, that the problem is more difficult with real data. One significant problem is the rate measurement. The ideal data included regularly spaced isochrons. Unfortunately, for time scales of only a few million years, the magnetic reversal time scale provides only a small number of isochrons spaced rather coarsely. The resulting limited resolution allows nonunique solutions for the propagation history.

PROPAGATION VELOCITY VARIATION

Propagating rifts are generally treated as quasi-steady state features, which, once initiated, move with constant velocity such that neither the direction nor rate change with time. Such models successfully predict the general geometries of the oblique linear seafloor features observed. Since these geometries are controlled by the rate and direction of both rift propagation and spreading, linear features are produced when these parameters remain constant over the time of rift propagation. A straightforward extension of these ideas is suggested by the observation of curved structures, which can be viewed as recording the variation of geometric factors such as the isochron reorientation or pseudofault angles, during the rift propagation time. Such variation, and hence curvature, is a natural consequence of any variation with time in the rate or direction of either rift propagation or spreading.

Since propagation velocity is a vector, either the rate (magnitude) or direction can change during propagation. Consider first the case where the propagation rate, but not the direction, changes. For convenience, we use the terms "acceleration" and "deceleration" to describe only rate, rather than direction, changes. For simplicity, both the obliquity and ridge-normal propagation velocity component are assumed to be zero. Figure 3 shows the evolution of a rift where propagation takes place with a constant rate from 1.0 to 0.5 Ma and then accelerates from 0.5 to 0.0 Ma. Velocity space diagrams illustrate the geometry at instants just before 0.5 and 0.0 Ma. Comparison of these two shows that increasing the propagation rate, with spreading rate held constant, causes the pseudofaults, failed rift, and isochrons in the transferred lithosphere to more closely parallel the growing ridge. The map views show the net result: comparison of the 0.5 and 0.0 Ma geometries shows that structures produced during the period of constant propagation rate are linear, and those from the period when the propagation rate was changing are curved. The spatial variation of the lineation curvature thus reflects the temporal variation of the propagation rate. Since the acceleration occurred gradually, the pseudofaults, failed rift, and reoriented isochrons acquire curvature away from the propagator. The outer pseudofault acquires the reverse curvature. Note that iso-

PROPAGATION ACCELERATION

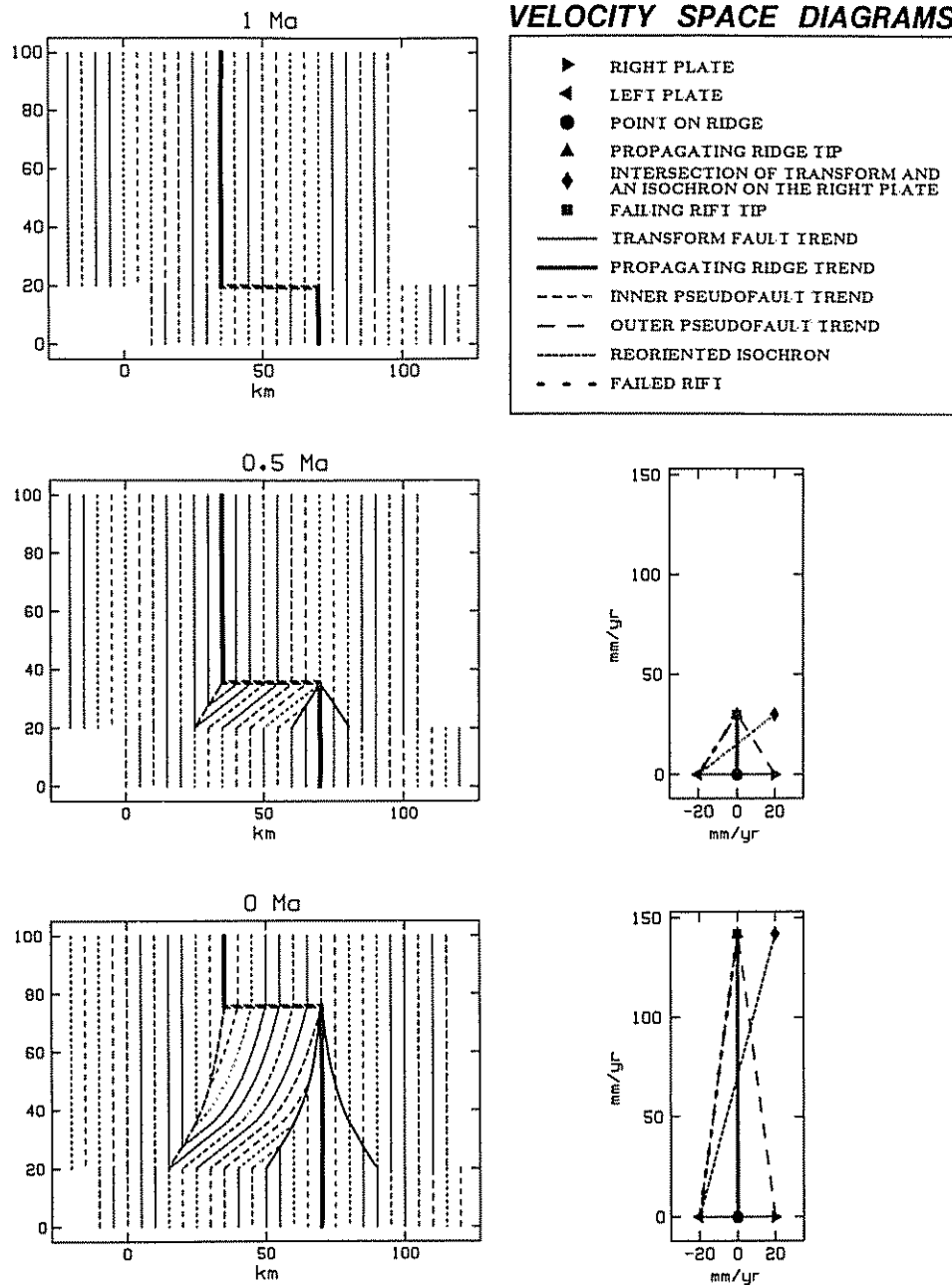


Fig 3. Rift propagation geometry resulting from increasing the propagation rate during the plate boundary evolution. Propagation begins at the southern ridge-transform intersection at 1 Ma. The propagation rate remains constant from 1 to 0.5 Ma and then increases gradually until 0 Ma. As a result of the acceleration, the pseudofaults, failed rift, and reoriented isochrons curve away from the propagator. Isochrons are created every 0.25 my. The velocity space diagrams represent the propagation configuration the instant before 0.5 and 0 Ma.

chrons produced on the growing ridge are not curved; their trend is that of the propagator, which is straight, since that direction was held constant.

Not surprisingly, propagation deceleration has the opposite effect. The propagator in Figure 4 has the same propagation and spreading rate from 1.0 to 0.5 Ma as in Figure 3, and then the propagation rate gradually decreases from 0.5 Ma to present. The propagation direction and the rate and azimuth of spreading remain constant. The gradual propagation deceleration yields pseudofaults, failed rift, and reoriented isochrons with curvature concave

toward the growing ridge. As before, isochrons produced on the growing ridge are straight.

The curvatures from the accelerating and decelerating propagators are not surprising. For small values of obliquity and ridge-normal propagation velocity the pseudofault angles (see notation list) depend on the ratio of half spreading rate u to ridge-parallel propagation rate v . Thus as a propagator decelerates, the ratio of the width of new lithosphere created to the distance the rift tip moves per unit time increases, so the pseudofaults curve toward the growing ridge. Similarly, since the ratio of displace-

PROPAGATION DECELERATION

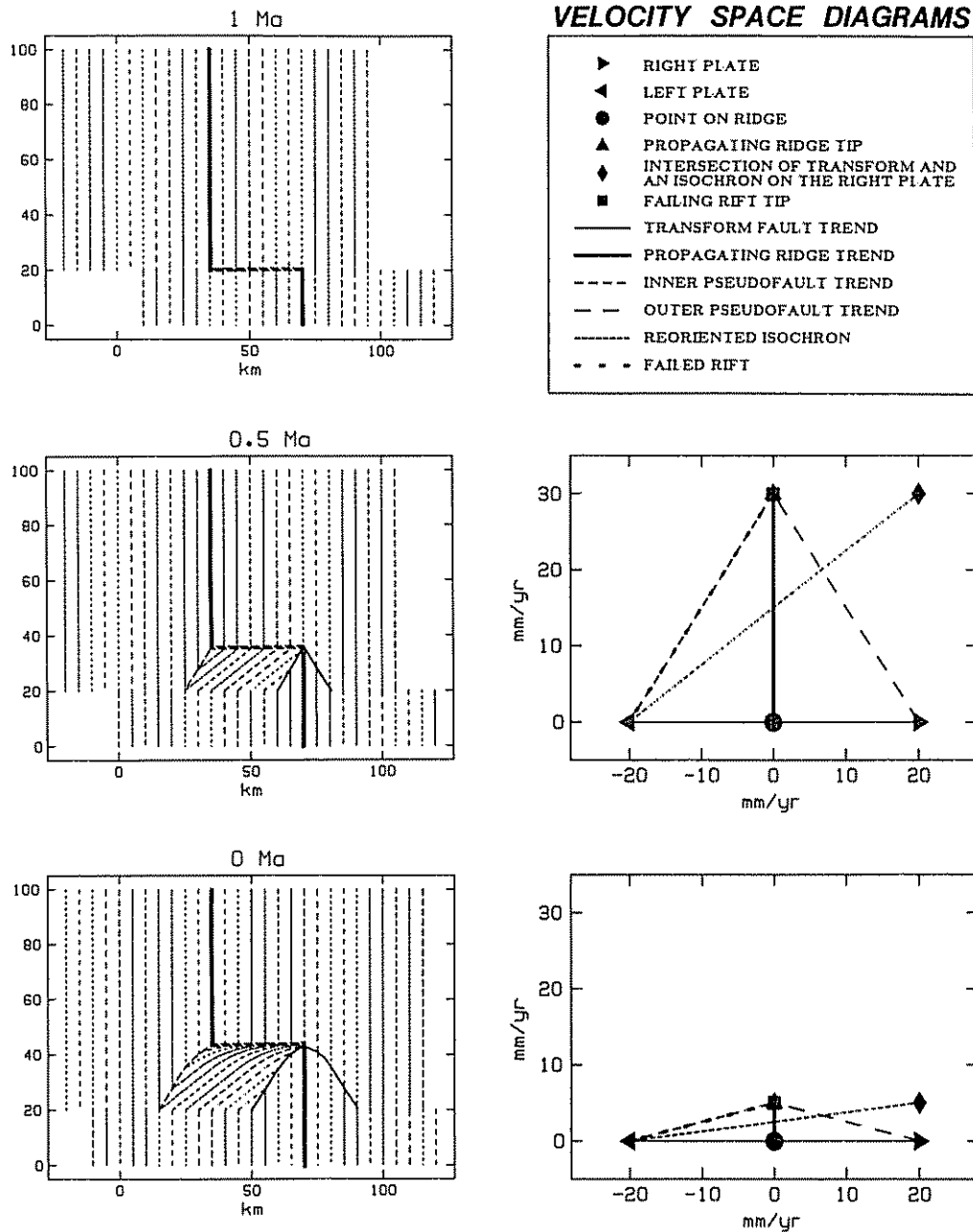


Fig. 4. Rift propagation geometry resulting from decreasing the propagation rate during the plate boundary evolution. Propagation begins at the southern ridge-transform intersection at 1 Ma. The propagation rate remains constant from 1 to 0.5 Ma and then decreases gradually until 0 Ma. As a result of the deceleration, the pseudofaults, failed rift, and reoriented isochrons curve toward the propagating rift. The isochron interval and times represented by the velocity space diagrams are the same as in Figure 3.

ment on the instantaneous transform to the distance the rift tip moves increases, the reoriented isochrons curve toward the growing ridge. The opposite situation occurs for an accelerating propagator.

An alternative style of propagation velocity variation is one in which the propagation rate is constant but the direction changes. Figure 5 shows a case in which the angle between the direction of propagation and the doomed ridge trend increases with time. The velocity space figures show that this corresponds to increasing the ratio of the ridge-normal (w) to ridge-parallel (v) com-

ponents of the propagation rate. The trends of the propagating rift, the isochrons created on it, and the pseudofaults all curve away from the doomed rift, and spreading on the new ridge becomes progressively more oblique. The reverse (Figure 6) occurs if the propagation direction turns toward the doomed rift. Interestingly, in either of the cases shown the reoriented isochrons and failed rift are curved slightly concave toward the propagator. The velocity space diagrams and the notation list indicate why this subtle change occurs. For small obliquities, the relevant angles α and β depend on the ratio of the spreading rate

DIRECTIONALLY VARYING PROPAGATOR

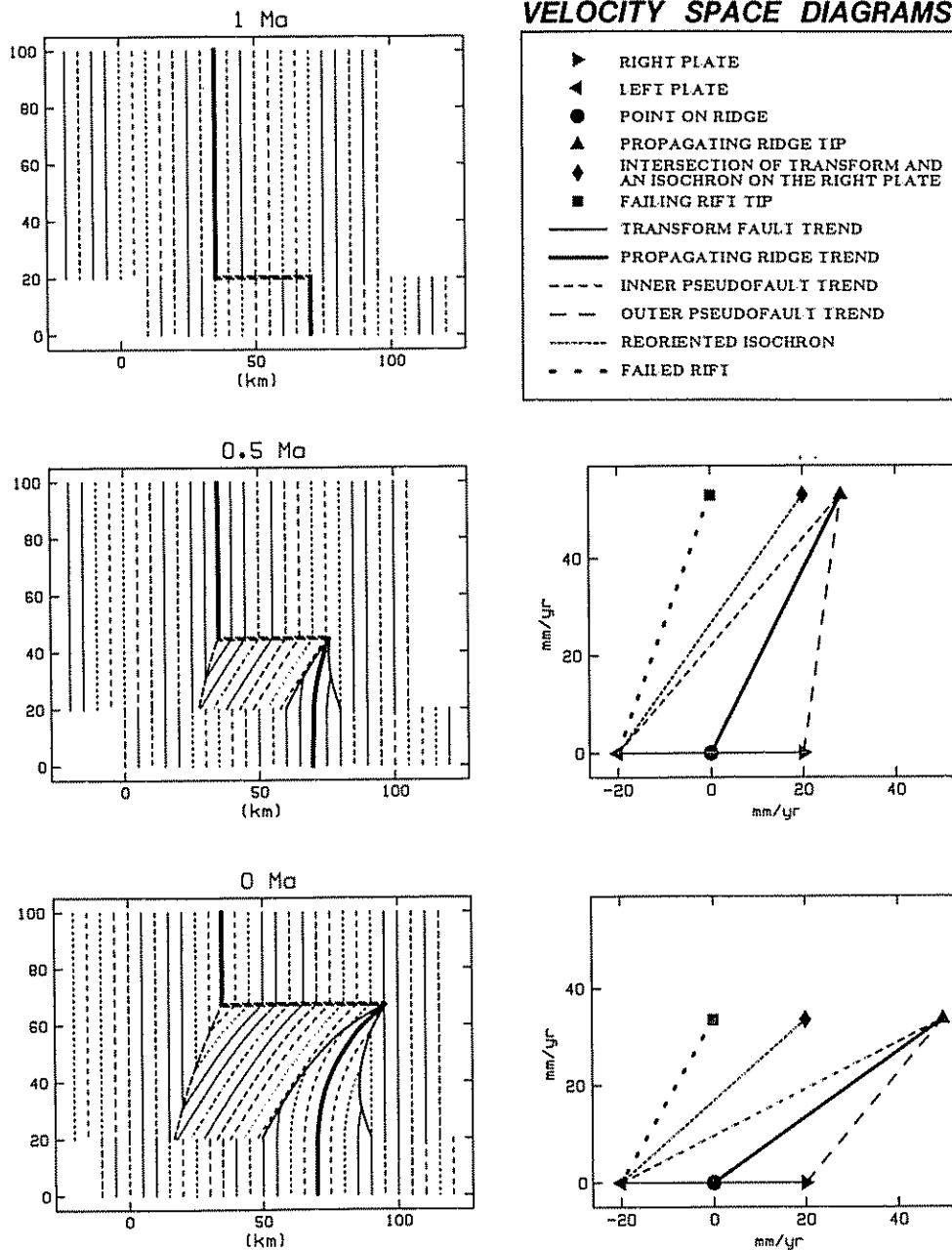


Fig. 5. Rift propagation geometry resulting from changing the propagation direction during the plate boundary evolution. Propagation begins at the southern ridge-transform intersection at 1 Ma. The propagation rate remains constant during the evolution, but with time the new rift diverges from the doomed one, breaking into successively older lithosphere. The resulting isochrons and pseudofaults curve away from the doomed rift. A slight curvature of the failed rift and reoriented isochrons away from the doomed rift results, since the ridge-parallel propagation component increases due to the directional change. The isochron interval and times represented by the velocity space diagrams are the same as in Figure 3.

to the ridge-parallel propagation rate. Since the magnitude of the propagation rate remained constant, either of the equal but opposite changes in propagation direction increases its ridge-normal component and thus decreases its ridge-parallel component.

It is useful to compare the overall effect of the four cases discussed so far. Acceleration or deceleration of the propagation rate alone causes the reoriented isochrons, failed rift, and pseudofaults to curve away from or toward the propagator. In these cases, isochrons formed at the

propagator do not curve. In contrast, changes in the propagation direction alone can cause the propagator, isochrons formed at it, and both pseudofaults to curve in the same direction, either away from or toward the doomed rift. In these cases, the reoriented isochrons and failed rift curve slightly toward the propagator. Thus although changes in either the propagation direction alone or in the propagation rate alone can produce grossly similar curved oblique fabric, the differences are adequate to discriminate the two.

DIRECTIONALLY VARYING PROPAGATOR

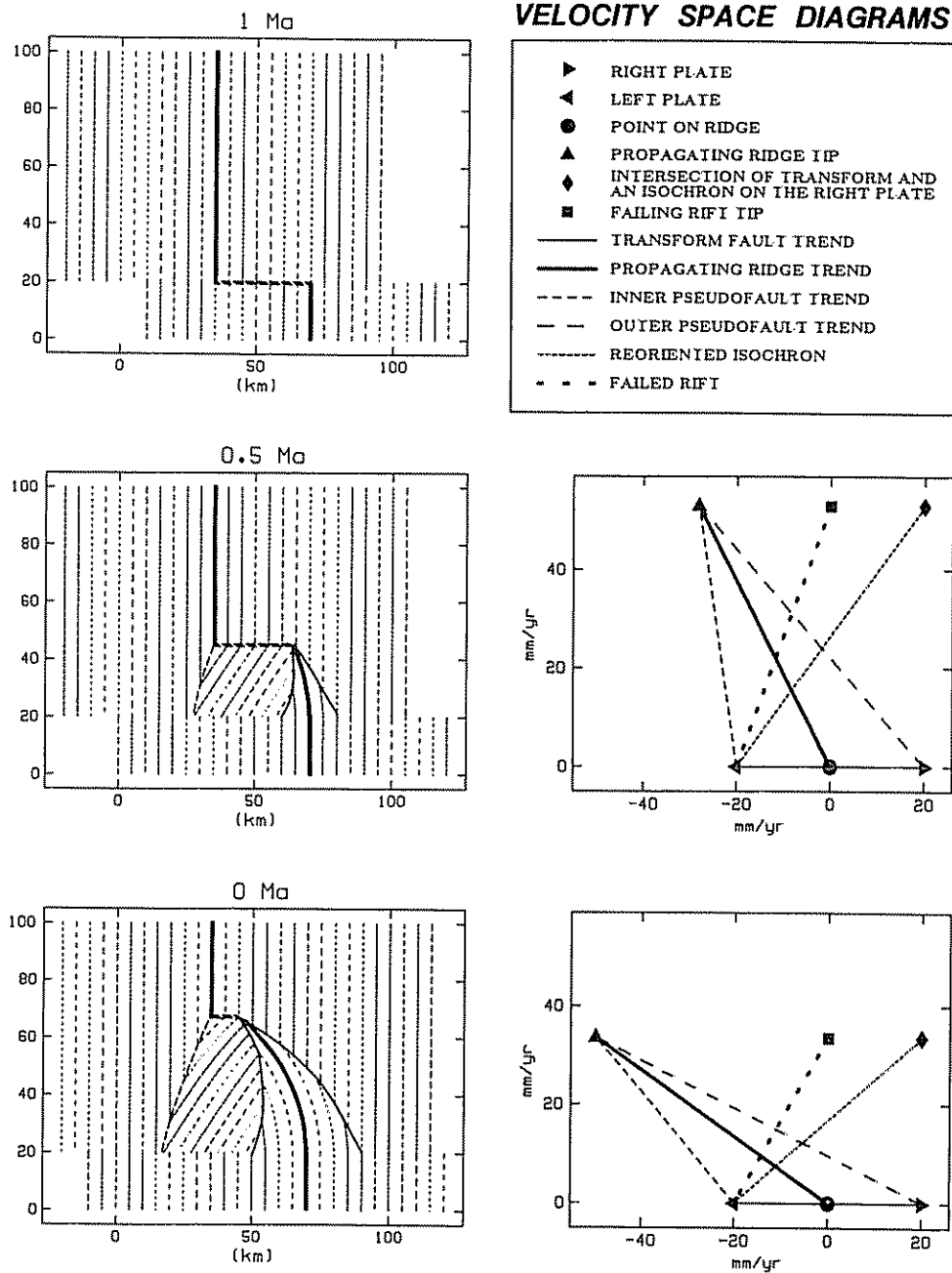


Fig. 6. Rift propagation geometry resulting from changing the propagation direction during the plate boundary evolution. The parameters are the same in Figure 5 except that the new rift turns toward the doomed one, growing in successively younger lithosphere. The resulting isochrons and pseudofaults curve toward from the doomed rift. The isochron interval and times represented by the velocity space diagrams are the same as in Figure 3.

SPREADING RATE AND DIRECTION CHANGES

Changes in the spreading rate during propagation can also result in curvature of the various tectonic elements. The results can be quite similar to those of propagation acceleration or deceleration. This is because, of the five angles characterizing the various tectonic elements, only the propagation direction does not depend somewhat on the ratio of half spreading rate to ridge-parallel propagation rate. As a result, increasing one has similar effects to decreasing the other. This trade-off becomes exact for zero obliquity and ridge-normal propagation rate, in which case

the lineation trends depend only on the ratio. To highlight this ambiguity, we show (Figures 7 and 8) spreading rate changes in a geometry such that the propagation direction is the same as in the acceleration and deceleration examples (Figures 3 and 4). Comparison of Figures 3 and 7 and Figures 4 and 8 illustrates the general similarities. Note that the latter cases differ in that the isochron spacing reflects the spreading rate change. In theory, then, curved fabric produced by spreading rate changes could be distinguished from that resulting from propagation rate changes by using isochrons to determine the spreading rate history. We will see, however, that this

INCREASING SPREADING RATE

VELOCITY SPACE DIAGRAMS

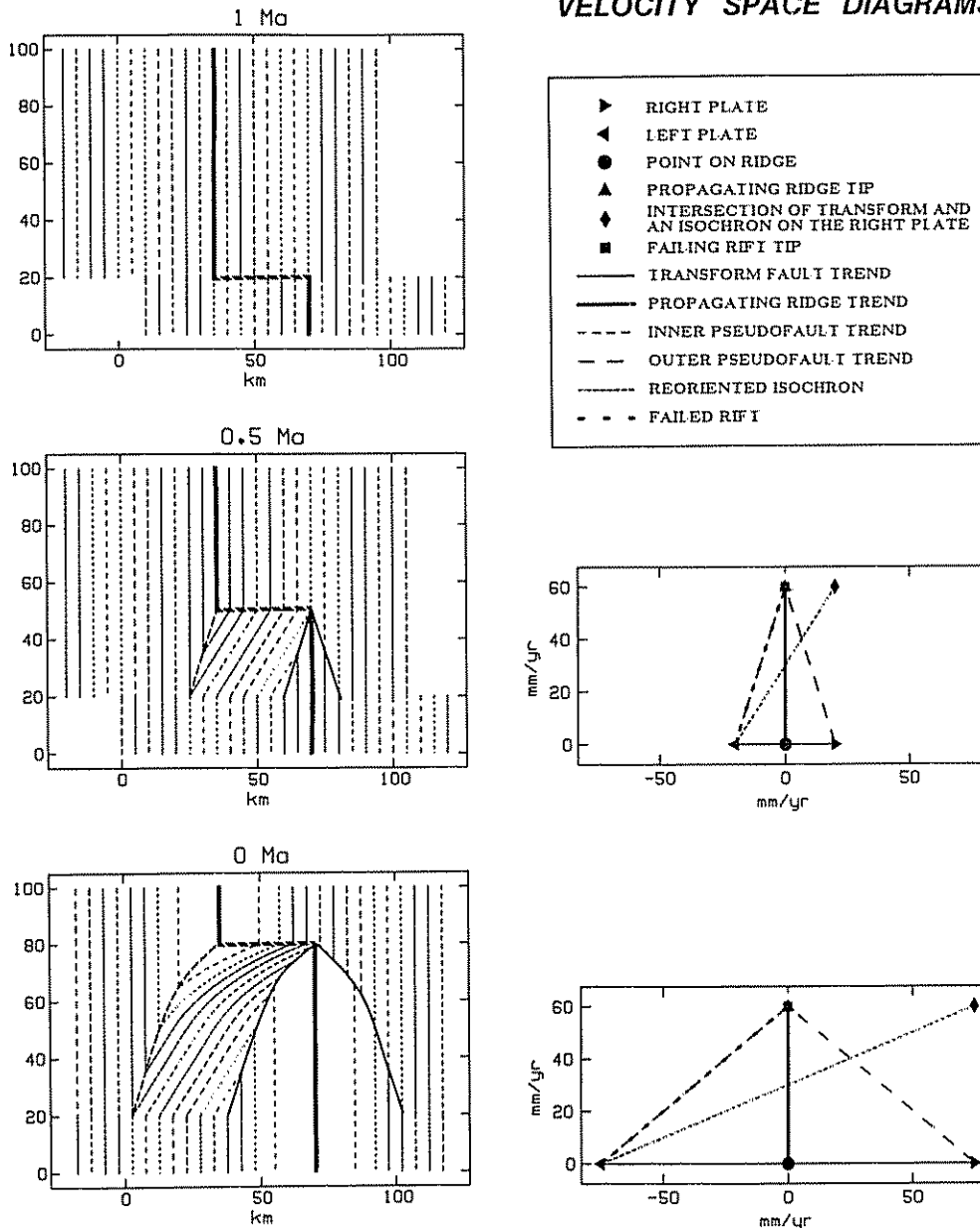


Fig 7. Rift propagation geometry resulting from increasing the spreading rate during the plate boundary evolution. Propagation begins at the southern ridge-transform intersection at 1 Ma. The spreading rate remains constant from 1 to 0.5 Ma and then increases gradually until 0 Ma. The resulting pseudofaults, failed rift, and reoriented isochrons curve toward the propagator. Note the similarity with the decelerating propagator case (Figure 4). These two effects can be distinguished from the distance between isochrons. The isochron interval and times represented by the velocity space diagrams are the same as in Figure 3.

may prove difficult if the magnetic anomaly isochrons are not adequately spaced. For example, at Galapagos, since either change would have occurred during the last few hundred thousand years, within the present period of normal polarity, both are consistent with the data.

As noted earlier, the geometry resulting from propagation also depends on the direction of spreading. Rift propagation often occurs in a geometry where the preexisting segments are spreading obliquely and the rift propagates at a different trend, such that spreading becomes more orthogonal [Hey, 1977]. This particular situation is illus-

trated in Figure 1, where the preexisting oblique spreading is replaced by orthogonal spreading on the propagator. In this case, θ which gives the obliquity, or spreading direction with respect to the doomed rift, remains constant.

A change in spreading direction would produce a new trend for some lineations, and consequently, varying the spreading direction over time can produce curved structures. Changes in spreading direction can generate curved lineations in two ways. Either the spreading direction could change during the propagation evolution, or the trend of the doomed rift that is eventually replaced by the

DECREASING SPREADING RATE

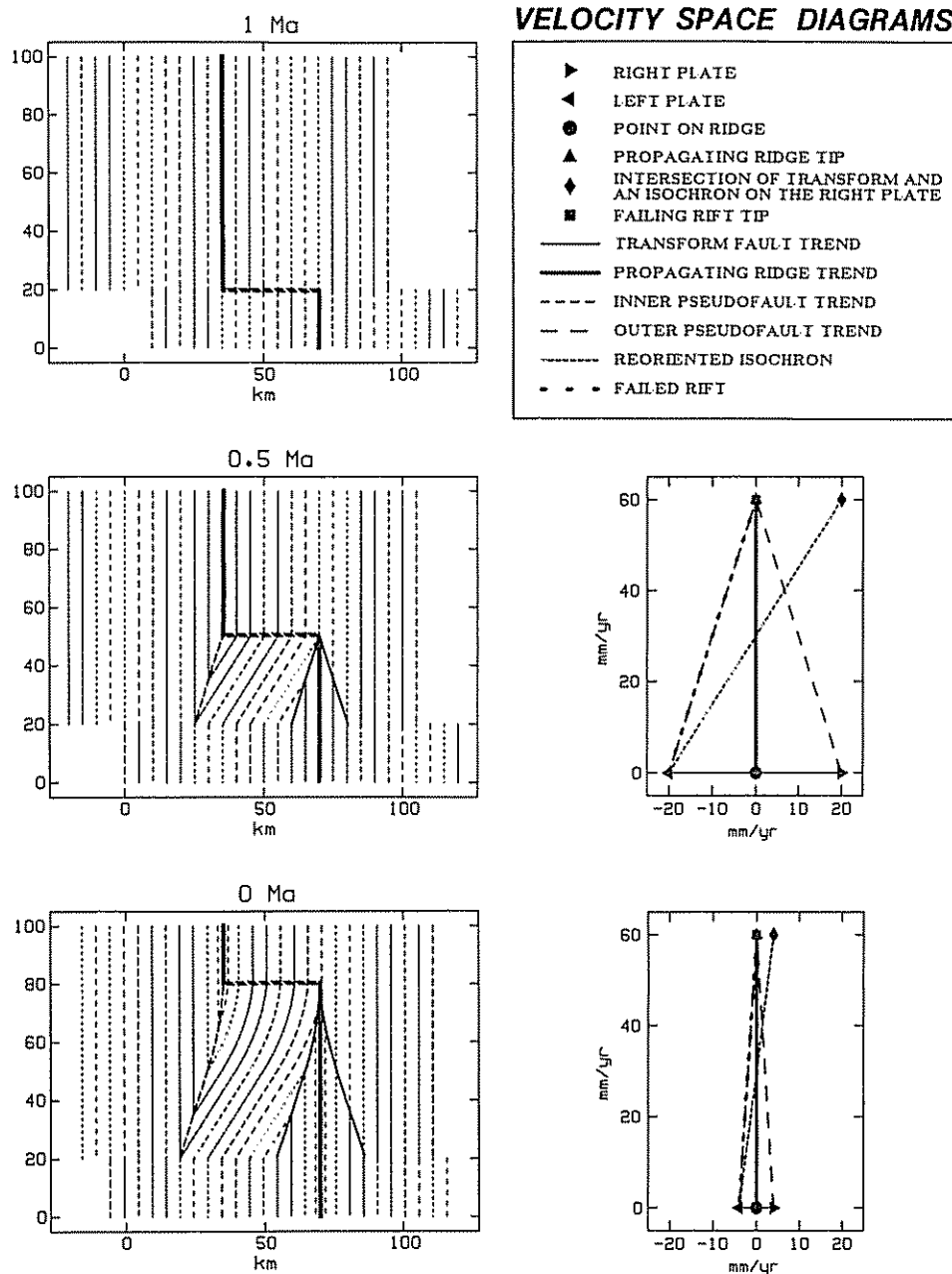


Fig. 8. Rift propagation geometry resulting from a slowing of spreading during the plate boundary evolution. Propagation begins at the southern ridge-transform intersection at 1 Ma. The spreading rate remains constant from 1 to 0.5 Ma and then decreases gradually until 0 Ma. The resulting pseudofaults, failed rift, and reoriented isochrons curve away from the propagator. Note the similarity with the accelerating propagator case (Figure 3). These two effects can be distinguished from the distance between isochrons. The isochron interval and times represented by the velocity space diagrams are the same as in Figure 3.

new ridge could vary over its original length. The first case is somewhat difficult to picture because the transform fault at the propagating rift tip would change its trend and cause lithosphere to be transferred from one plate to the other. Some pieces of lithosphere could be transferred back and forth between the two plates several times, presumably resulting in a distorted lineation pattern. The second case is less interesting because the curved lineations would result from an originally curved divergent plate boundary. This case should be easy to detect because

anomalies created by the curved spreading center would retain that shape even outside the zone of transferred lithosphere.

THE 95° 5' W GALAPAGOS PROPAGATOR

The propagating rift at 95° 5' W on the Nazca-Cocos plate boundary is the best studied example of presently active rift propagation. Surveys here, showing seafloor fabric curving away from the propagator and toward the

GALAPAGOS ACCELERATING PROPAGATOR

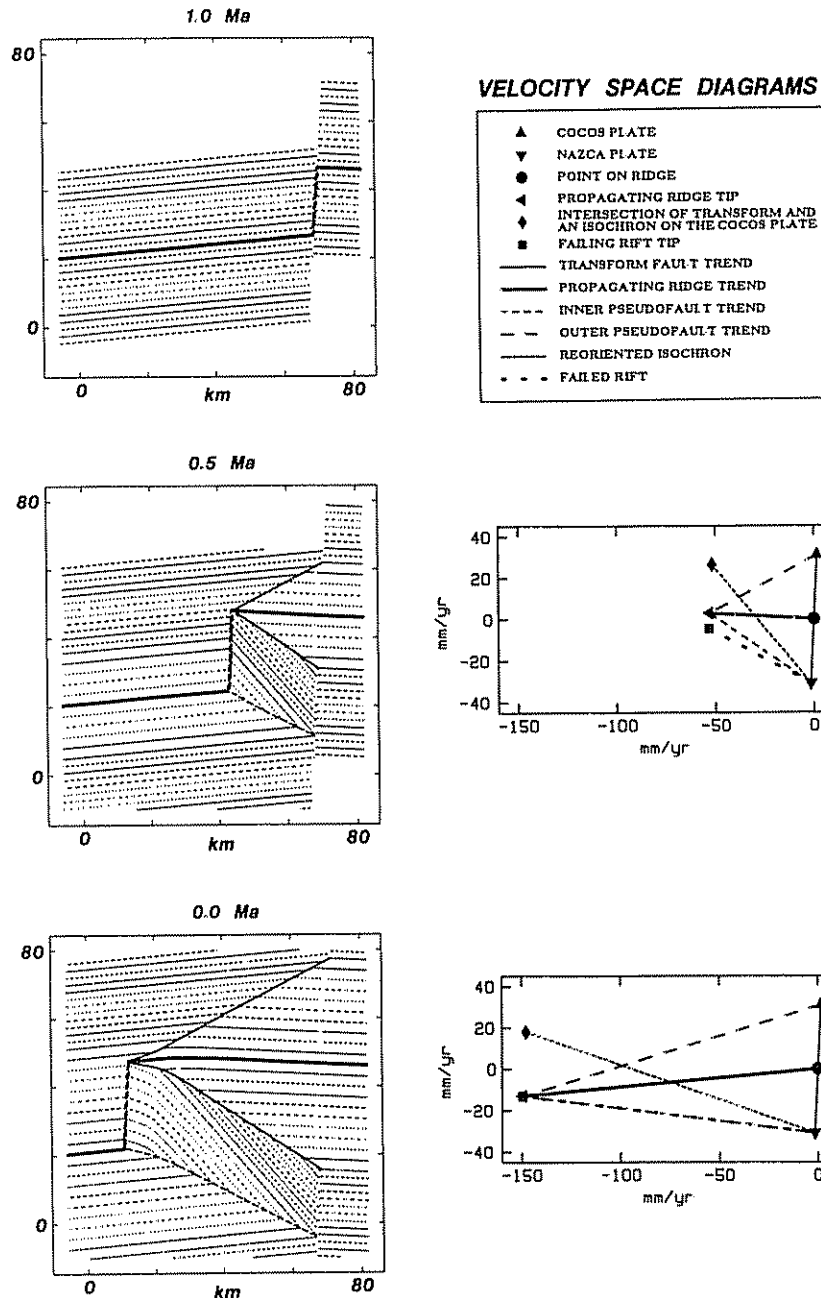


Fig 9. Accelerating propagator model for the Galapagos propagator. Propagation begins at the eastern ridge-transform intersection at 1 Ma. The propagation rate and direction and spreading history are given in Figure 11. As a result of the acceleration, the pseudofaults, failed rift, and reoriented isochrons curve away from the propagator. Isochrons are created every 0.1 m.y. The velocity space diagrams represent the propagation configuration the instant before 0.5 and 0 Ma.

failed rift, provide the observations interpreted as requiring a shear zone between the two rifts and hence a local deviation from rigid plate tectonics. Given that we have seen that curved seafloor fabric can be generated by a variety of models based entirely on rigid plate tectonics, we now investigate whether such models can replicate the observations. In this undertaking, we are guided by the principle that the models be constructed consistent with the geophysical data as interpreted by the original investigators, rather than our own reinterpretation, unless otherwise noted. We thus briefly review these data and interpretations (Figure 2), as given by Hey et al [1986]

The present propagating rift tip is located at $\sim 2^{\circ} 38' N, 95^{\circ} 32' W$. Hey et al [1986] refer to this as the tectonic tip, where the pseudofaults converge, and suggest that the volcanic tip lags behind to the SE. The propagating ridge has an azimuth of $\sim 265^{\circ}$ from the tectonic tip to $95^{\circ} 23' W$ where it then bends to an average azimuth of 277° to the edge of our study area ($95^{\circ} 05' W$). The lineations created on the propagating ridge essentially parallel the ridge axis. The inner and outer pseudofaults that bound this lithosphere have respective azimuths of 122° and 64° east of the rift tip and 99° and 70° near the tip. The failed rift indicates the past position of the

doomed rift and separates transferred lithosphere to the north from normal lithosphere to the south. It is located to the south of the "sinuous scarp" and has an average azimuth of $117^\circ \pm 5^\circ$.

A trend of $\sim 265^\circ$ is inferred for the doomed rift throughout the propagation history from the trend of the magnetic lineations created by it. During the propagator's evolution, lithosphere was transferred from the Cocos plate to the Nazca plate. The resulting lineations in the transferred lithosphere have an average azimuth of $145^\circ \pm$

10° east of $95^\circ 25' W$. To the west, they exhibit obvious curvature and trend nearly E-W as they approach the inferred present transform.

As discussed later, our two models incorporate different propagation and spreading rate histories. Except when otherwise indicated, we use propagation rates similar to the 52 mm/yr given by *Hey et al* [1986] and full spreading rates of 50 mm/yr for 4.0 to 0.7 Ma and 30 mm/yr for 0.7 Ma to the present from *Hey et al* [1980].

We have developed two rift propagation models for this

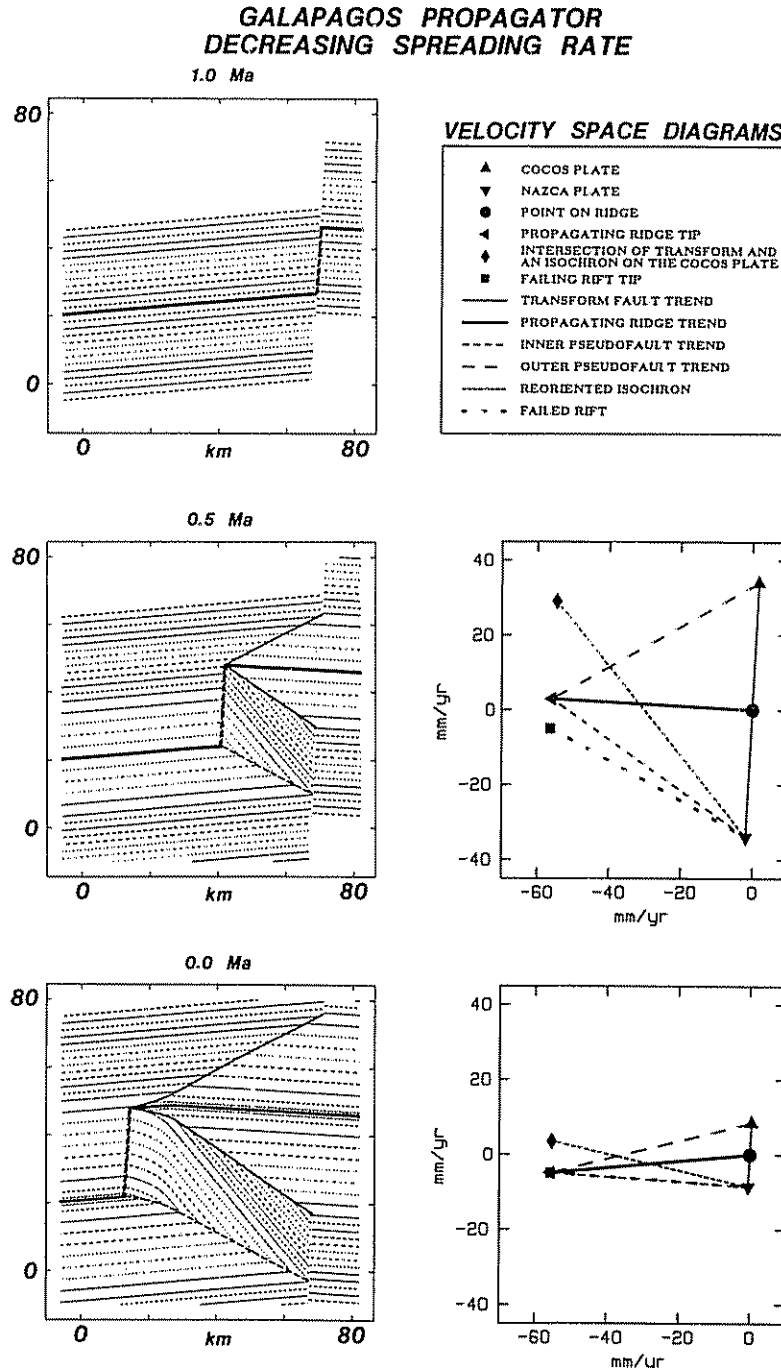


Fig 10. Decreasing spreading rate model for the Galapagos propagator. Propagation begins at the eastern ridge-transform intersection at 1 Ma. The propagation rate and direction and spreading history are given in Figure 11. As a result of the spreading rate decrease, the pseudofaults, failed rift, and reoriented isochrons curve away from the propagator. Isochrons are created every 0.1 m.y. The velocity space diagrams represent the propagation configuration the instant before 0.5 and 0 Ma.

area, one with an accelerating propagator (Figure 9) and one with a decreasing spreading rate (Figure 10) Both models are intended as schematic, rather than as reconstructions Our goal is to show that such rift propagation histories and geometries, which are consistent with the available tectonic constraints, can generate the observed curved lineation pattern with no deviation from rigid plate tectonics

Both models have the same, somewhat arbitrary, initial configuration of a single transform offsetting two ridge segments The offset is chosen to place the failed rift trend along that observed in the present geometry Although no well-defined transform fault can be delineated from the data, we place a transform with a 3° azimuth at the propagating rift tip The eastern segment then propagates westward, causing migration of the transform and instantaneous cessation of spreading on the preempted portions of the western segment Spreading on the east segment is assumed to be orthogonal, thus parallel to the transform orientation; the west segment is given a different trend (265°) and thus spreads obliquely We then trace the evolution of this system for 1 m.y., using two different rift propagation and spreading rate histories (Figure 11)

We regard our models as successful to the extent that they replicate the general character of the present seafloor fabric and marine magnetic data (Figure 12) The lineations observed on the Sea Beam image are assumed to represent isochrons comparable to those predicted by the models The predicted magnetic anomalies are generated using isochrons at 0-73, 92-95, and 1.67-1.87 Ma to

represent the Brunhes normal polarity chron and Jaramillo and Olduvai normal polarity events [Cox and Hart, 1986]

In general, the fits are good Several points are worth noting At Galapagos the doomed rift is offset to the south of the scarp thought to be the trace of the failed rift; the models did not include this effect and for simplicity treated the doomed rift as a single ridge segment The fits to the west of this offset are thus not as good We similarly did not attempt to model or resolve the origin of the systematic difference between the lineation orientation (essentially east-west) and the magnetic anomaly orientation (265°) north of the propagating and dying rifts

The spatial variation in the seafloor fabric presumably reflects temporal variation in the propagation process Since the curved lineations occur in a region within 20 km of the present rift tip, they would be expected to result from a change in either propagation or spreading rate within the last few hundred thousand years (Figures 11 and 12) In contrast, the linear structures further east presumably reflect an earlier period of essentially uniform propagation and spreading rate Thus the reason that both models fit the general character of the observations is that the primary difference between them is the position of the isochrons formed during the period of propagation acceleration or spreading rate decrease The trends of the isochrons are quite similar Given that the last isochron recorded by a magnetic reversal is at 0.73 Ma, the magnetic anomaly patterns resulting from the different propagation and spreading histories during the latter portion of the present (Brunhes) normal polarity chron are quite simi-

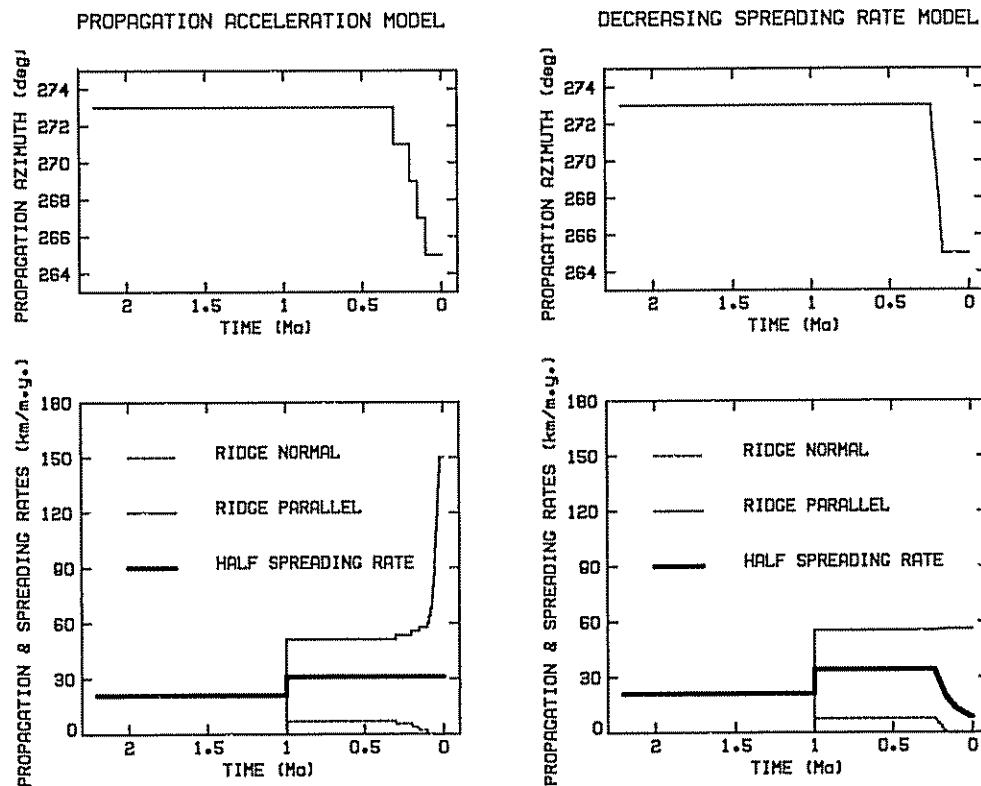


Fig. 11. Propagation and spreading history (left) for the Galapagos accelerating propagator model of Figure 9, and (right) for the Galapagos decreasing spreading rate model of Figure 10 The two top figures show the azimuth of rift propagation for the respective models, and the bottom figures give the ridge-normal and ridge-parallel propagation velocity components, and half spreading rates. Spreading direction was assumed constant for the doomed rifts.

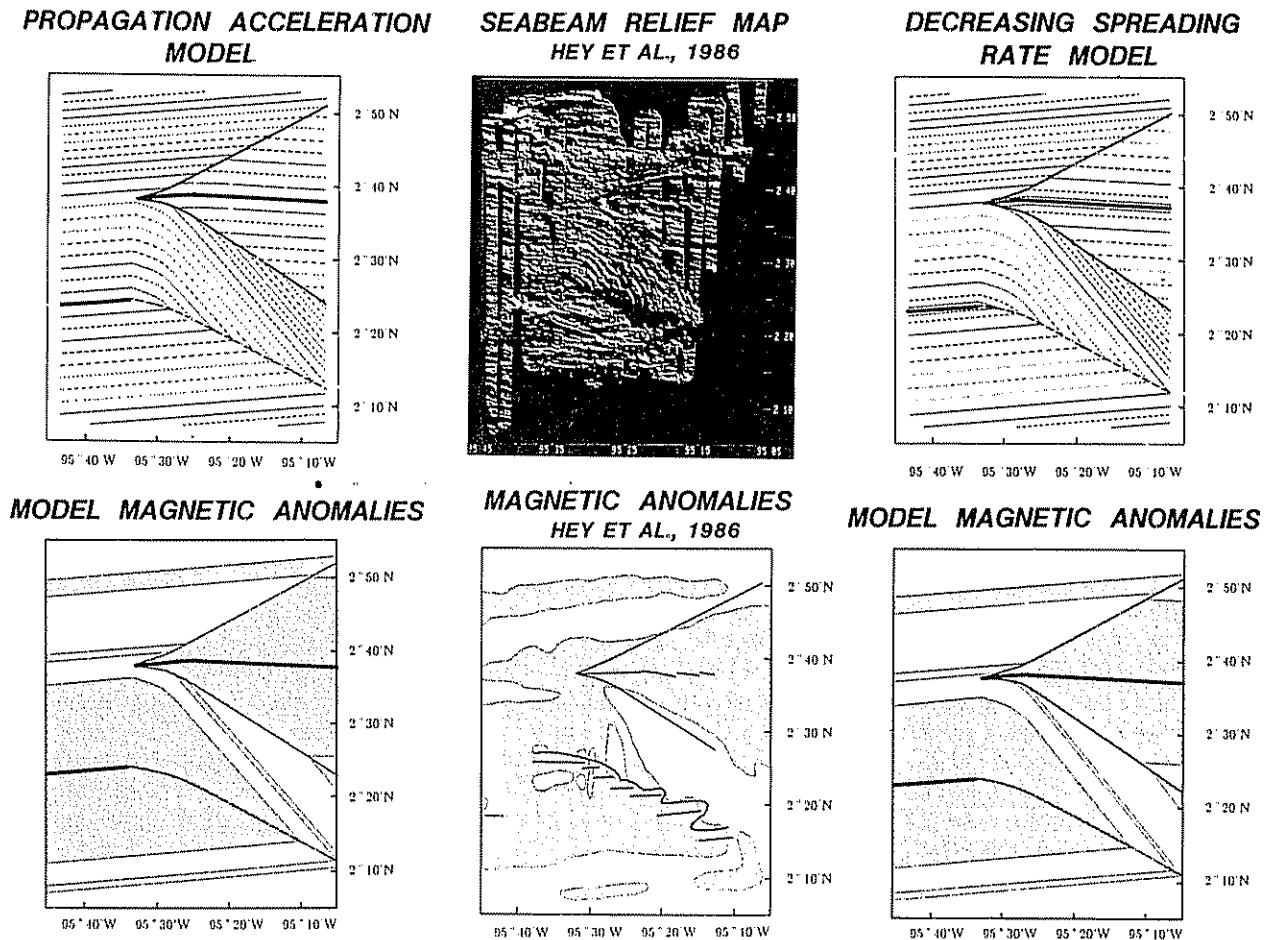


Fig. 12 Comparison of the present seafloor fabric and marine magnetic data to predictions of the Galapagos accelerating propagator model (Figure 9) and of the Galapagos decreasing spreading rate model (Figure 10). The general character of the seafloor fabric and magnetics is successfully reproduced.

lar For the same reason, they are similar to a magnetic block model [Miller and Hey, 1986] with constant propagation and spreading rates

DISCUSSION

We conclude that the curved lineations which have been interpreted as requiring a shear zone between the growing and dying rifts are equally consistent with models which do not deviate from purely rigid plate tectonics. Discrimination between rigid plate and shear zone models for the Galapagos propagator thus seems difficult. Figure 13 illustrates this point; comparison of a line drawing of the structural data, as interpreted by McKenzie [1986], to the predictions of his shear zone model and one of our rigid plate models shows that the latter fits the data at least as well as the former. The similarity of the rigid and shear models' predictions occurs, since in the shear model the spreading rate on the propagator is zero at the tip and increases with distance, an effect similar to a rigid model in which the spreading rate has been decreasing with time.

Since both the different rigid plate models and the shear zone model fit the magnetic and lineation data for the Galapagos 95° W propagator, it appears difficult to determine which model is more suitable. The rigid and shear models differ in their description of the fine-scale nature of the plate boundary. On a large scale the relative motion

between plate pairs, in this case Nazca and Cocos, is described by a rigid plate model. It is clear that rift propagation must be added to the model to describe the overall change in spreading center geometry. An appealing aspect of the rift propagation hypothesis is that it allows the overall change in spreading center geometry to be described with only a minor addition to a rigid plate tectonic model, that of a time-variable boundary configuration. The question is then what modifications are needed to describe the curved structures.

The assumption of a time-variable rate is a natural one, since nothing in the rift propagation hypothesis requires that propagation occur at a constant rate. Searle and Hey [1983] suggested this possibility for the 95° W propagator, based on the changes in pseudofault directions. Similarly, rift propagation models for the Juan de Fuca [Wilson et al., 1984] and Gorda [Stoddard, 1987] ridges incorporate variable propagation rates. Moreover, since changes in plate motion rates are a normal feature of the rigid plate model, the assumption of a decrease in spreading rate represents no additional hypothesis. Alternatively, the shear zone model requires a local deviation from rigid plate tectonics.

A possible argument for a distributed shear zone at Galapagos is the observation of diffuse microseismicity between the growing and dying rifts [Cooper et al., 1987]. Despite the uncertainties in location of microearthquakes

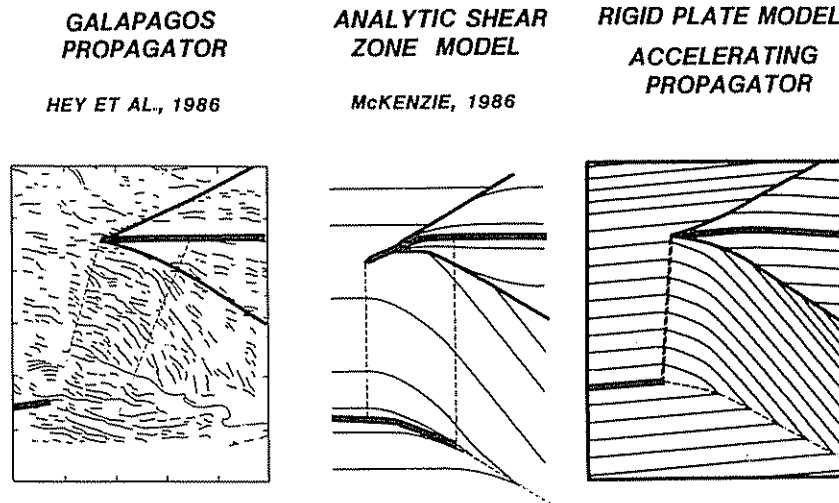


Fig. 13. Comparison of the Galapagos seafloor fabric (line drawing from McKenzie [1986], based on Searle and Hey [1983] and Hey *et al.* [1986]) to the predictions of a shear zone model and of the accelerating propagator model (Figure 9). The decreasing spreading rate model would look similar (Figure 10). Since the rigid plate models fit at least as well as the shear model, the curved lineations need not indicate a departure from purely rigid plate tectonics.

in such a complex region using laterally homogeneous velocity models [Trehu and Solomon, 1983], it seems likely that microseismicity is scattered within the curved lineation region. This region is a complex one for either of the propagator models; in one it is actively shearing and in the other it has been disrupted by the transform migration. It is thus possible to conceive of a number of different tectonic models consistent with the observed microseismicity [Cooper *et al.*, 1987].

It may, however, be possible to discriminate between rigid plate and shear zone models using observations at other propagators. One test would be to seek evidence of deceleration and acceleration on other propagators from periods where the magnetic reversal time scale allows the necessary resolution. Other tests could be done with fabric observations at additional propagators. The shear model requires that the lineation and rift tip curvature observed here be a feature of all active propagators. Similarly, such curvature, which represents a transient effect, should be observed only near the tips of active propagators. In contrast, observation of fabric with a variety of orientations, including reverse curvature consistent with propagation deceleration, and linear fabric consistent with constant velocity propagation, would favor the rigid plate tectonic model. Furthermore, in this model, curvature might be observed on no longer active propagators. A test for a recent spreading rate decrease would be if other propagators on the Cocos-Nazca boundary show similar curvature. Thus although nonunique interpretations are possible, observations at other propagators may be quite valuable. It may well be the case that different propagators behave quite differently. In particular, it may be some time before it is clear how generally conclusions from the Galapagos apply to other propagators.

As both the rigid plate models and the shear zone model are kinematic ones, neither offers direct insight into the dynamics of rift propagation. The kinematics, once understood, should provide useful constraints on dynamic models [Phipps Morgan and Parmentier, 1985].

Resolution of whether the region between growing and dying rifts acts rigidly or shears could also have implications for microplate studies. Although estimates of the areas associated with individual regions bounded by dual spreading centers are somewhat model dependent, since spreading at even a single ridge occurs over a finite distance and can be complicated, dual ridge systems appear to span a broad spatial range (Figure 14). Overlapping spreading centers (OSCs), where two ridges are resolvable, have linear dimensions of kilometers and areas of tens of kilometers [Macdonald and Fox, 1983; Sempere and Macdonald, 1986]. At a somewhat larger scale, features associated with the Galapagos and Cobb [Johnson *et al.*, 1983; Karsten *et al.*, 1986] propagating rift systems cover areas of hundreds of kilometers. The Easter and Juan Fernandez plates are larger overlap regions with areas of $10^4 - 10^5$ km². Fossil microplates include the Bauer [Mammerickx *et al.*, 1980], Tula (between Pacific and Aluk) [Cande *et al.*, 1982], Chinook [Rea and Dixon, 1983], and Magellan [Tamaki and Larson, 1988] plates. Finally, although definition of the largest scale is also somewhat arbitrary, a useful index is the Cocos plate (3×10^6 km²), which is commonly treated as a small major plate. In a very general way, the rigidity of the overlap region may correlate with its size. If an overlap region on this 10- to 20-km scale acts as a rigid plate, it seems even more plausible that a microplate with a scale of hundreds of kilometers acts rigidly. The alternative, that an overlap region on this 10- to 20-km scale acts as a shear zone, is more difficult to derive larger-scale implications from. Such an observation may indicate that this is the scale at which rigid plate tectonics breaks down, in which case, larger overlap regions may nonetheless act rigidly. Alternatively, shear models might also be required for the larger "microplates."

AFTERWORD

This paper is submitted to the *Journal of Geophysical Research* issue in memory of Allan Cox. Geophysics is the

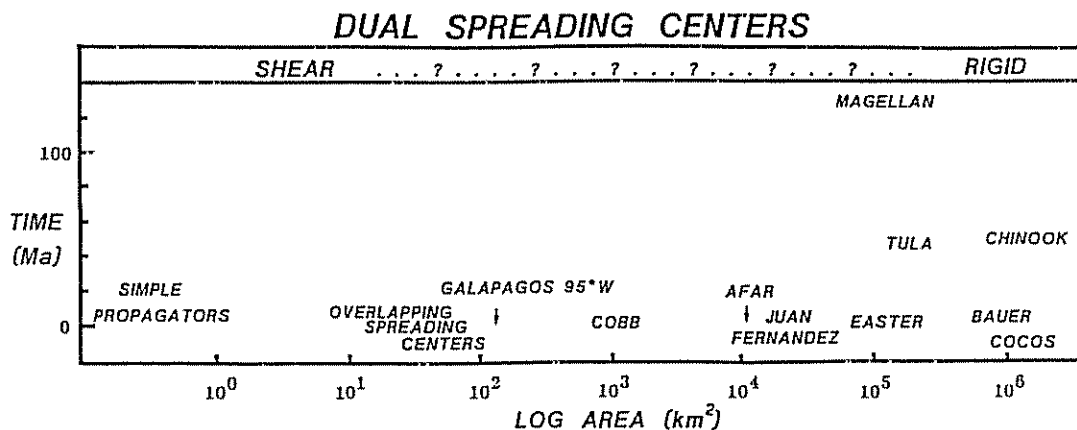


Fig. 14. Areas of various overlap regions and the time at which they are last thought to have acted as independent entities. When several estimates for the area have been given, the largest value is shown. Overlap region rigidity may vary with region size.

poorer for the loss of his insight and spirit. We have benefited from fruitful discussions with him during our studies of oceanic spreading center evolution. Thus in investigating the possible applicability of rigid plate tectonics to rift propagation, we have attempted to follow the spirit Allan described in his recent book:

A subliminal goal is to convey some of the playfulness and lightness that characterized early research in plate tectonics. Now that plate tectonics has become a serious subject, it's hard to remember why we had so much fun doing plate tectonics.

Plate Tectonics: How It Works
Allan Cox and Robert B. Hart

NOTATIONS

The following symbols are used to describe the propagating rift geometries (see also Figure 1)

- u half spreading rate normal to doomed rift
- v propagation velocity component parallel to doomed rift
- w propagation velocity component normal to doomed rift
- α acute angle between trend of failed rift and doomed rift
- β acute angle between trend of reoriented isochron and doomed rift
- λ acute angle between trend of propagating ridge and doomed rift
- μ acute angle between trend of inner pseudofault and doomed rift
- ϵ acute angle between trend of outer pseudofault and doomed rift
- θ obliquity of doomed rift

Velocity Space Points and Coordinates

- Z origin (0, 0)
- A left plate ($-u, u \tan \theta$)
- B right plate ($u, -u \tan \theta$)
- D dying rift tip ($0, v + w \tan \theta$)
- P propagating rift tip (w, v)
- R reoriented isochron-transform intersection ($u, v + (w - u) \tan \theta$)

Geometric Relationships

$$\alpha = \tan^{-1} \{ u / [v + (w - u) \tan \theta] \}$$

$$\beta = \tan^{-1} \{ 2u / [v + (w - 2u) \tan \theta] \}$$

$$\lambda = \tan^{-1} (w / v)$$

$$\mu = \tan^{-1} \{ (u + w) / (v - u \tan \theta) \}$$

$$\epsilon = \tan^{-1} \{ (u - w) / (v + u \tan \theta) \}$$

Acknowledgements. The computer code used to model rift propagation was developed by John Werner. We thank Richard Hey, Roger Searle, and Paul Stoddard for useful discussions, and Hans Schouten and an anonymous reviewer for helpful comments. This research was supported by NSF grant EAR 8618038 and NASA Crustal Dynamics contract NAS5-27238. Acknowledgement is also made to the donors of the Petroleum Research Fund, administered by the American Chemical Society, for partial support of this research.

REFERENCES

- Anderson, R. N., D. W. Forsyth, P. Molnar, and J. Mammertickx, Fault plane solutions of earthquakes on the Nazca plate boundaries and the Easter plate, *Earth Planet. Sci. Lett.*, **24**, 188-202, 1974.
- Anderson-Fontana, S., J. F. Engeln, P. Lundgren, R. L. Larson, and S. Stein, Tectonics and evolution of the Juan Fernandez microplate at the Pacific-Nazca-Antarctic triple junction, *J. Geophys. Res.*, **91**, 2005-2018, 1986.
- Cande, S. C., E. M. Herron, and B. R. Hall, The early Cenozoic history of the southeast Pacific, *Earth Planet. Sci. Lett.*, **57**, 63-74, 1982.
- Cooper, P. A., P. D. Milholland, and F. K. Duennebier, Seismicity of the Galapagos 95.5°W propagating rift, *J. Geophys. Res.*, **92**, 14,091-14,112, 1987.
- Courtillot, V., A. Galdeano, and J. L. Le Mouel, Propagation of an accreting plate boundary: A discussion of new aeromagnetic data in the Gulf of Tadjurah and southern Afar, *Earth Planet. Sci. Lett.*, **47**, 144-160, 1980.
- Cox, A., and R. B. Hart, *Plate Tectonics: How it Works*, 392 pp., Blackwell Scientific Publications, Palo Alto, 1986.
- Engeln, J. F., and S. Stein, Tectonics of the Easter plate, *Earth Planet. Sci. Lett.*, **68**, 259-270, 1984.
- Engeln, J. F., S. Stein, J. Werner, and R. G. Gordon, Microplates and shear zone models for oceanic spreading center reorganization, *J. Geophys. Res.*, **93**, 2839-2856, 1988.
- Forsyth, D. W., Mechanisms of earthquakes and plate motions in the East Pacific, *Earth Planet. Sci. Lett.*, **17**, 189-193, 1972.
- Francheteau, J., A. Yelles-Chaouche, and H. Craig, The Juan Fernandez microplate near the Pacific-Nazca-Antarctic plate junction at 35°S, *Earth Planet. Sci. Lett.*, **86**, 253-268, 1987.
- Handschumacher, D. W., R. H. Pilger, Jr., J. A. Foreman, and J.

- F. Campbell, Structure and evolution of the Easter plate, *Mem. Geol. Soc. Am.*, 154, pp. 63-76, 1981.
- Herron, E. M., Sea-floor spreading and the Cenozoic history of the east-central Pacific, *Geol. Soc. Am. Bull.*, 88, 1671-1691, 1972a
- Herron, E. M., Two small crustal plates in the South Pacific near Easter Island, *Nature Phys. Sci.*, 240, 35-37, 1972b
- Hey, R., A new class of "pseudofaults" and their bearing on plate tectonics: A propagating rift model, *Earth Planet. Sci. Lett.*, 37, 321-325, 1977
- Hey, R., and P. Vogt, Spreading center jumps and sub-axial asthenosphere flow near the Galapagos hotspot, *Tectonophysics*, 37, 41-52, 1977.
- Hey, R. N., and D. S. Wilson, Propagating rift explanation for the tectonic evolution of the Northeast Pacific-The pseudomovie, *Earth Planet. Sci. Lett.*, 53, 167-188, 1982
- Hey, R., F. K. Duenebier, and W. J. Morgan, Propagating rifts on mid-ocean ridges, *J. Geophys. Res.*, 85, 3647-3658, 1980.
- Hey, R. N., D. F. Naar, M. C. Kleinrock, W. J. P. Morgan, E. Morales, and J.-G. Schilling, Microplate tectonics along a superfast seafloor spreading system near Easter Island, *Nature*, 317, 320-325, 1985.
- Hey, R. N., M. C. Kleinrock, S. P. Miller, T. M. Atwater, and R. C. Searle, Sea Beam/Deep-Tow investigation of an active oceanic propagating rift system, Galapagos 95.5° W, *J. Geophys. Res.*, 91, 3369-3393, 1986
- Johnson, H. P., J. L. Karsten, J. R. Delaney, E. E. Davis, R. G. Currie, and R. L. Chase, A detailed study of the Cobb offset of the Juan de Fuca Ridge: Evolution of a propagating rift, *J. Geophys. Res.*, 88, 2297-2315, 1983.
- Karsten, J. L., S. R. Hammond, E. E. Davis, and R. G. Currie, Detailed geomorphology and neotectonics of the Endeavour Segment, Juan de Fuca Ridge: New results from Seabeam swath mapping, *Geol. Soc. Am. Bull.*, 97, 213-221, 1986.
- Macdonald, K. C., and P. J. Fox, Overlapping spreading centres: New accretion geometry on the East Pacific Rise, *Nature*, 302, 55-58, 1983
- Mammerickx, J., E. Herron, and L. Dorman, Evidence for two fossil spreading ridges in the southeast Pacific, *Geol. Soc. Am. Bull.*, 91, 263-271, 1980.
- McKenzie, D. P., The geometry of propagating rifts, *Earth Planet. Sci. Lett.*, 77, 176-186, 1986.
- Menard, H. W., T. E. Chase, and S. M. Smith, Galapagos rise in the southeast Pacific, *Deep Sea Res.*, 11, 233-244, 1964
- Miller, S. P., and R. N. Hey, Three-dimensional magnetic modeling of a propagating rift, Galapagos 95° 30' W, *J. Geophys. Res.*, 91, 3395-3406, 1986.
- Morgan, W. J., Rises, trenches, great faults, and crustal blocks, *J. Geophys. Res.*, 73, 1959-1982, 1968.
- Naar, D. F., and R. N. Hey, Fast rift propagation along the East Pacific Rise near Easter Island, *J. Geophys. Res.*, 91, 3425-3438, 1986.
- Phipps Morgan, J., and E. M. Parmentier, Causes and rate-limiting mechanisms of ridge propagation: A fracture mechanics model, *J. Geophys. Res.*, 90, 8603-8612, 1985.
- Rea, D. K., and J. M. Dixon, Late Cretaceous and Paleogene tectonic evolution of the North Pacific Ocean, *Earth Planet. Sci. Lett.*, 65, 145-166, 1983.
- Schilling, J.-G., H. Sigurdsson, A. N. Davis, and R. N. Hey, Easter microplate evolution, *Nature*, 317, 325-331, 1985.
- Searle, R. C., and R. N. Hey, Gloria observations of the propagating rift at 95.5° W on the Cocos-Nazca spreading center, *J. Geophys. Res.*, 88, 6433-6448, 1983.
- Sempere, J.-C., and K. C. Macdonald, Deep-tow studies of the overlapping spreading centers at 9° 03' N on the East Pacific Rise, *Tectonics*, 5, 881-900, 1986.
- Stoddard, P. R., A kinematic model for the evolution of the Gorda plate, *J. Geophys. Res.*, 92, 11,524-11,532, 1987.
- Tamaki, K., and R. L. Larson, The Mesozoic history of the Magellan microplate in the western central Pacific, *J. Geophys. Res.*, 93, 2857-2874, 1988.
- Trehu, A. M., and S. C. Solomon, Earthquakes in the Orozco transform zone: Seismicity, source mechanisms and tectonics, *J. Geophys. Res.*, 88, 8203-8225, 1983.
- Wilson, D. S., R. N. Hey, and C. Nishimura, Propagation as a mechanism of reorientation of the Juan de Fuca Ridge, *J. Geophys. Res.*, 89, 9215-9225, 1984.

G. Acton and S. Stein, Department of Geological Sciences, Northwestern University, Evanston, IL 60208.

J. F. Engeln, Department of Geology, University of Missouri, Columbia, MO 65211.

(Received September 21, 1987;
revised March 16, 1988;
accepted March 30, 1988)